

# **Reliable Voltage Monitoring System for Synchronization of Distributed Power Generation Systems to Utility Grid**

**A thesis submitted to the Department of Electrical Engineering (Power  
Electronics & Drives) in partial fulfillment of the requirements for the degree  
of Master of Technology**

**By**

**SAROJ KUMAR PANDA  
Roll No: 212EE4249**



**DEPARTMENT OF ELECTRICAL ENGINEERING  
NATIONAL INSTITUTE OF TECHNOLOGY, ROURKELA  
PIN-769008, ODISHA  
(2012-2014)**

# **Reliable Voltage Monitoring System for Synchronization of Distributed Power Generation Systems to Utility Grid**

**A thesis submitted to the Department of Electrical Engineering (Power  
Electronics & Drives) in partial fulfillment of the requirements for the degree  
of Master of Technology**

**By**

**SAROJ KUMAR PANDA**

**Roll No: 212EE4249**

**Under the guidance of**

**PROF. S. GOPALAKRISHNA**



**DEPARTMENT OF ELECTRICAL ENGINEERING  
NATIONAL INSTITUTE OF TECHNOLOGY, ROURKELA  
PIN-769008, ODISHA  
(2012-2014)**

*Dedicated to*  
*My mother & My Motherland (Bharat)*



National Institute of Technology, Rourkela

## *Certificate*

This is to certify that the thesis entitled, “Reliable Voltage Monitoring System for Synchronization of Distributed Power Generation Systems to utility grid” submitted by Saroj Kumar Panda in partial fulfillment of the requirements for the award of Master of Technology Degree in Electrical Engineering with specialization of “*Power Electronics & Drives*” at the National Institute of Technology, Rourkela is an authentic work carried out by him under my supervision and guidance.

To the best of my knowledge, the matter embodied in the thesis has not been submitted to any other University/ Institute for the award of any degree or diploma.

Date:

**Prof. S. Gopalakrishna**

Assistant professor

Place:

**Department of Electrical Engineering**

**National Institute of Technology**

**Rourkela - 769008**

## Acknowledgement

My sincere thanks to my guide **Prof. S. Gopalakrishna**, for his valuable guidance and constant support. I extend my thanks to our HOD, **Prof.A.K.Panda** for his valuable advices, and to our PG-Coordinator **Prof.K.B.Mohanty** for his cooperation and encouragement, I also thank all the teaching and non-teaching staff for their cooperation to the students.

My special thanks to **Prof.B.Chitti Babu** for his valuable suggestions and instruction. I also thank all my friends, without whose support, my life might have been miserable here.

I wish to express my thankfulness to my parents, my friends, whose love and inspiration have reinforced me throughout my education.

Finally I dedicated all to this **land**, and this is not other than India, my India.

.

**Saroj Kumar Panda**

# ABSTRACT

The unceasing progression of DPGS (Distributed Power Generation Systems) gives an effective and inexpensive approach, for electricity generation near by the consumer. Though for better performance, the distributed power generating stations are being allied to the utility network, there is an emergent necessity for the DPGS to work properly and uninterruptedly in case small grid instabilities. This needs developments to be made for the control arrangement of DPGSs at the grid-side converter. As a consequence, grid interlinking necessities applied to distributed generations, are need to be continuously updated for maintaining the stability and the quality of the grid voltage. In the realm of grid interconnection, grid synchronization system is the main part of the control scheme of grid connected inverter. This is liable for extracting the phase angle of the grid voltage. One best technique, which is used today are phase-locked loops.

From the beginning of the thesis a brief introduction about the distributed power generating stations is given. Later, voltage monitoring systems based on zero crossing detection (ZCD) to Phase Locked Loop (PLL) are given. A comprehensive survey about quadrature-signal generation, which is essential for three-phase and single-phase phase-locked-loop, is given. These QSG techniques are investigated and simulated in MATLAB-2010. Finally, thesis covers an advance synchronization approach in both three-phase and single-phase PLL with the inclusion of Second Order Generalized Integrator (SOGI). Both PLLs are experimentally verified by the use of LABVIEW-2010 with coalition with NI USB 6341.

# Table of contents

<b>Abstract</b>	<b>i</b>
<b>Table of contents</b>	<b>ii</b>
<b>List of Figures</b>	<b>iv</b>
<b>List of Symbols</b>	<b>vi</b>
<b>List of Abbreviation</b>	<b>ix</b>
<b>Chapter 1 Introduction</b>	<b>2</b>
<b>1.1</b> Background and Inspiration	2
<b>1.1.1</b> Overview of Distributed Power Generating Stations	2
<b>1.1.2</b> Project motivation	3
<b>1.2</b> Objective	3
<b>1.3</b> Thesis outline	4
<b>Chapter 2</b> <b>Need of grid synchronization</b>	<b>6</b>
<b>Chapter 3</b> <b>Voltage monitoring system</b>	<b>8</b>
<b>3.1</b> Introduction	8
<b>3.2</b> Overview of grid voltage monitoring system	9
<b>3.2.1</b> Voltage monitoring based on ZCD	10
<b>3.2.2</b> Voltage monitoring based on PLL	11
<b>3.2.2.1</b> Zero Crossing Detection based PLL	12
<b>3.2.2.2</b> Arctangent Function based PLL	12

3.2.2.3	Park's Transform based PLL	13
3.3	Sequence components separation	15
3.3.1	Sequence components separation in three phase system	15
3.3.2	Sequence components separation in two phase system	16
3.4	Overview of QSG technique	18
3.4.1	Transport delay based QSG	19
3.4.2	Sampling and trigonometric function based QSG	19
3.4.3	Estimated phase angle and amplitude based QSG	21
3.4.4	SOGI based QSG	23
3.5	Single phase PLL	26
3.6	Three phase PLL	29
<b>Chapter 4</b>	<b>Conclusion</b>	<b>34</b>
4.1	Summery	34
4.2	Scope for Future work	34
<b>Bibliography</b>		<b>35</b>



# List of Figures

<b>Figure.1.</b>	<b>Maximum trip time with respect to both voltage amplitude and frequency, according to the standard IEC61727-2002 especially for PV systems.</b>	<b>09</b>
<b>Figure.2.</b>	<b>Classification of the grid voltage monitoring techniques for DPGS.</b>	<b>10</b>
<b>Figure.3.</b>	<b>Grid voltage monitoring based on Zero-Crossing Detection</b>	<b>11</b>
<b>Figure.4.</b>	<b>PLL structure by the use of Zero Crossing Detection</b>	<b>12</b>
<b>Figure.5.</b>	<b>PLL structure by the use of Arctangent Function</b>	<b>12</b>
<b>Figure.6.</b>	<b>PLL structure by the use of Park's Transformation matrix</b>	<b>14</b>
<b>Figure.7.</b>	<b>+Ve and -Ve sequence voltage orientation</b>	<b>16</b>
<b>Figure.8.</b>	<b>Input and Quadrature signal generated by QSG</b>	<b>18</b>
<b>Figure.9.</b>	<b>QSG constructed upon Transport Delay</b>	<b>19</b>
<b>Figure.10.</b>	<b>Input (blue) and Quadrature signal (red) generated by Transport Delay based QSG</b>	<b>19</b>
<b>Figure.11.</b>	<b>Quadrature signal generator based on trigonometric function and sampling delay</b>	<b>20</b>
<b>Figure.12.</b>	<b>Input (blue) and Quadrature (red) signal generated by sampling and trigonometric function based QSG</b>	<b>21</b>
<b>Figure.13.</b>	<b>Estimated phase angle and amplitude based OSG</b>	<b>21</b>
<b>Figure.14.</b>	<b>Phase of input supply, extracted by the single phase PLL in estimated phase angle and amplitude based QSG</b>	<b>22</b>
<b>Figure.15.</b>	<b>Amplitude of input supply, extracted by the single phase PLL in estimated phase angle and amplitude based QSG</b>	<b>22</b>

<b>Figure.16.</b>	<b>Input (blue) and Quadrature (red) signal generated by estimated phase angle and amplitude based QSG</b>	<b>22</b>
<b>Figure.17.</b>	<b>Frequency adaptive second order generalized integrator (SOGI)</b>	<b>23</b>
<b>Figure.18.</b>	<b>The SOGI-FLL, for a single-phase grid synchronization system</b>	<b>25</b>
<b>Figure.19.</b>	<b>Bode plot of the FLL input variables <math>E(s)</math> and <math>Q(s)</math></b>	<b>26</b>
<b>Figure.20.</b>	<b>Enlarge view of FLL</b>	<b>26</b>
<b>Figure.21.</b>	<b>Complete structure of single-phase PLL</b>	<b>27</b>
<b>Figure.22.</b>	<b>Input supply*230 given to single-phase PLL</b>	<b>28</b>
<b>Figure.23.</b>	<b>Filtered in-phase signal (<math>dV'</math>) and filtered quadrature signal (<math>qV'</math>) generated by SOGI-QSG</b>	<b>28</b>
<b>Figure.24.</b>	<b>Frequency tracked by SOGI-FLL</b>	<b>28</b>
<b>Figure.25.</b>	<b>Normalized in-phase component and extracted phase angle of the fundamental supply voltage</b>	<b>28</b>
<b>Figure.26.</b>	<b>Dual-SOGI synchronization system</b>	<b>30</b>
<b>Figure.27.</b>	<b>Experimental set-up</b>	<b>30</b>
<b>Figure.28.</b>	<b>2-phase input supply (<math>\alpha\beta</math>) to D-SOGI</b>	<b>31</b>
<b>Figure.29.</b>	<b>Frequency extracted by SOGI-FLL</b>	<b>31</b>
<b>Figure.30.</b>	<b>Extracted positive sequence fundamental components (<math>v_{\alpha}^{+}, v_{\beta}^{+}</math>)</b>	<b>32</b>
<b>Figure.31.</b>	<b>Extracted phase of +VE sequence fundamental component with respect to <math>v_{\alpha}^{+}</math></b>	<b>32</b>
	<b>*5</b>	<b>32</b>

## List of Symbols

$\omega$	Angular frequency of Input supply
$\omega^*$	Detected angular frequency
$t$	Time
$f$	Frequency of input supply
$f^*$	Detected frequency
$\omega_I$	Initial frequency value
$\varepsilon_\theta$	Phase error to PI controller
$\theta$	Phase of input supply
$\theta^*$	Detected phase
$V_{abc}$	Three phase input supply
$V$	Input Supply
$V_\alpha$	In-phase component of Input supply
$V_\beta$	Quadrature component of Input supply

$[P]$	Park's transformation matrix
$[T_{\alpha\beta}]$	Clarke's transformation matrix
$N$	Number of samples per a complete cycle
$V_d$	Direct axis component in rotating reference frame
$V_q$	Quadrature axis component in rotating reference frame
$V_{abc}^+$	Three phase +ve sequence components
$V_{abc}^-$	Three phase -ve sequence components
$V_{\alpha\beta}^+$	Two phase +ve sequence components
$V_{\alpha\beta}^-$	Two phase -ve sequence components
$\lambda$	Phase shift operator $1\angle 120^\circ$
$q$	Phase shift operator $1\angle -90^\circ$
$\gamma$	Phase delay/ Gain
$\tau$	Time delay
$A$	Amplitude

$\omega'$	Resonance frequency
$V'$	Filtered in-phase component
$qV'$	Quadrature component of filtered in-phase component
$\varepsilon_V$	Voltage error variable
$\varepsilon_f$	Frequency error variable
$D(s)$	Transfer function of $V'$ to $V$
$Q(s)$	Transfer function of $qV'$ to $V$
$E(s)$	Transfer function of $\varepsilon_V$ to $V$

## **List of Abbreviation**

<b>DPGS</b>	<b>Distributed Power Generating Station</b>
<b>WT</b>	<b>Wind Turbine</b>
<b>PV</b>	<b>Photovoltaic</b>
<b>FC</b>	<b>Fuel-cells</b>
<b>QSG/OSG</b>	<b>Quadrature/Orthogonal Signal Generator</b>
<b>SOGI</b>	<b>Second Order Generalized Integrator</b>
<b>PLL</b>	<b>Phase Locked Loop</b>
<b>ZCD</b>	<b>Zero Crossing Detection</b>
<b>PI</b>	<b>Proportional Integral</b>
<b>FLL</b>	<b>Frequency Locked Loop</b>
<b>M-SOGI</b>	<b>Multiple Second Order Generalized Integrator</b>
<b>LABVIEW</b>	<b>Laboratory Virtual Instrument Engineering Workbench</b>
<b>NI</b>	<b>National Instrument</b>
<b>USB</b>	<b>Universal Serial Bus</b>
<b>SRF</b>	<b>Synchronous Reference Frame</b>
<b>PSC</b>	<b>Positive Sequence Calculator</b>

*Chapter 1*  
*(Introduction)*

# Introduction

In the initial phase of chapter, the background and inspiration for the thesis are given. Then, the main objective behind the thesis with a small overview of Distributed Power Generation Systems (DPGS) is elaborated. Finally, the thesis is outlined in a clear manner.

## 1.1 Background and Inspiration

Due to the rapid growth in load, demands put on conventional power systems are increasing throughout the world. These demand made the engineer to think more, for the renewable energy source. But when we are concerning about distribution systems due to the disperse population, the same engineer are thinking for the distributed power sources.

In old-fashioned power systems, buck amount of power is produced at a comparatively less number of power plants. These plants are remote to the consumers. Generally generators in these power stations are working at pre-defined constant rotor speed, which depend upon the grid frequency. In these power-plants, stepping-up of the voltage is done before transmission, and stepping-down of voltage occur just after the transmission or before utilization.

But due to the limited stock of fossil fuel and deep concern towards green technology, renewable sources are become in-evitable choice over the traditional power-plant. For example, as on or before 2007, power generation based on Wind turbines (WT) and photovoltaic (PV), have seen dynamic growth in that decade [1], [2]. These small-scale electricity generating systems are also known as Distributed Power Generating Stations (DPGS). DPGS makes it possible, to generate electricity near to the utility grid or load(s). For better efficiency and reliable power supply, these Generating Stations need to be interconnected, with the utility grid. A single phase Distributed Power Generating Stations, briefly presented in following section.

### 1.1.1 Overview of Distributed Power Generating Stations (DPGS)

In traditional power systems, mostly the electricity is generated in a large amount. And the centralized power stations, which is placed at a far distance from the utility grid. On a contrary, the Distributed Power Generating Stations generate electricity in a less amount and used nearby. That could be specifically beneficial to consumers, who reside in country-sides with inadequate access to consistent and undisrupted energy sources. These DPGSs mainly generate electricity for homes, office, industries etc. As a result, the complete organization of the power system has started changing, due to the rapid growth of DPGSs [3], [4], [5].



Interfacing of DPGS with the utility grid is frequently done. So, when there is a lack of electricity, the users can still get electricity from the distribution network. And when there is excess of electricity, the surplus amount exported to utility grid. DPGS could be able to generate electricity, by using different systems, including both exhaustible and inexhaustible sources. These different systems are Photo-Voltaic Generators, Wind-Turbines (WT), Wave Generators, Fuel-Cells (FC), Small Hydro and gas/steam power stations. But the connection of DPGSs to the utility grid is only possible, when the power level of DPGS is below 5kW, like Photo Voltaic and Fuel Cell. But it is important to note, recent power systems should have the capability in providing consistent power supply as old-fashioned power systems. Also it should be in same cost, for making the grid interfacing of DPGS an affordable choice.

Renewable energy sources are facing some problem, due to its high cost and their dependency on weather pattern. Consumer demand may not match with the availability of these energies. Additional worry is that, power can flow in both direction in case of grid-interconnected DPGS. The flow of reactive power in both directions can cause voltage oscillation, which create instability of the utility grid. But bi-directional power flow is not intended to accommodate with the grid. So it must be cautiously accomplished by well-designed controllers.

### **1.1.2 Project motivation**

Distributed power generating stations are useful, for the promotion of renewable energy sources over conventional fossil fuels. Due to its onsite generation and consumption, it directly improves the efficiency of the electricity network by reducing the transmission and distribution loss. Green technology is also one of its advantages.

Apart from all these advantages, distributed generation also put forth some new challenges towards the researcher. Among these challenges, the main attention has been given toward it interfacing with utility grid. Interfacing of harmonics, in between distributed grid connected power converter and the distribution network, has been articulated [6]. So to preserve the quality and stability of utility network, grid interconnection requirements should be uninterruptedly updated with the condition of the grid [7-11].

## **1.2 Objective**

The main aim of this thesis is to investigate different types of grid voltage monitoring systems, in order to give an uninterrupted service with the coalition of utility grid, under grid

abnormalities. Regarding the detection of the grid voltage, it mainly has three aspects for detection, namely: amplitude, frequency and phase. To pledge the exact reference signals generation and to meet the load demand, the grid-connected inverters need a correct and fast estimation of the amplitude, frequency and phase angle of the grid voltage. But by the instability in the grid, the grid voltage condition monitoring system is affected a lot, and provides inaccurate values for controlling purpose. So there may have a chance of undesired disconnections and poor performance of the DPGS. Therefore, we investigated a number of reliable systems for grid voltage monitoring. Moreover, the explained systems are having a fast detection rate and showing robustness under grid disturbances.

### **1.3 Thesis outline**

This thesis is completely divided in to four chapters.

Chapter 1 briefly shows the challenges to modern power system, while interfacing the DPGSs to the utility grid. A review of the basic control necessities for the grid connected DPGS is done in this chapter. In what aspect grid synchronization is important to control the grid-connected DPGS, is also briefly illustrated. Finally, the objective of the thesis and motivation behind the project are given.

Chapter 2 is completely dedicated to the necessity of grid voltage monitoring in power system.

From the beginning of Chapter 3, a brief introduction about the distributed power generating stations is given. Later, voltage monitoring systems based on zero crossing detection (ZCD) to Phase Locked Loop (PLL) are given. A comprehensive survey about quadrature-signal generation, which is essential for three-phase and single-phase phase-locked-loop, is given. These QSG techniques are investigated and simulated in MATLAB-2010. Then, thesis covers an advance synchronization approach in both three-phase and single-phase PLL with the inclusion of Second Order Generalized Integrator (SOGI). Finally both PLLs are experimentally verified by the use of LABVIEW-2010 with coalition with NI USB 6341.

Chapter 4 gives a conclusion to the thesis, including the possible suggestions for future work.

## *Chapter 2*

### *(Need of grid synchronization)*

## **Need of grid synchronization**

A strong grid synchronization technique is a central part of grid connection requirement to achieve better controllability. It is largely accountable for detecting the phase angle of the utility grid, to which the DPGS going to be interfaced. Later this phase angle is used for the synchronization of DPGS's control variables. Synchronization of DPGS to utility grid is an advantageous approach irrespective of stand-alone system. Apart from its on-site use, it is convenient for the DPGS, to send the surplus of power to utility grid. Therefore, it improves the efficiency of the distributed generation [12]. At the time of grid disturbance like failure of generating station, these DPGSs able to provide the lack of power to the national grid, if it is properly synchronize with the grid [13]. Many other advantages like economic, provision of green technology, multifariousness uses of electricity and safe power supply are also possible by this synchronization [14]. Furthermore, synchronization is also needed for the study of electrical power quality [15].

*Chapter 3*  
*(Voltage monitoring system)*

## **Voltage monitoring system**

This chapter starts with a small summary about grid voltage condition monitoring techniques. Following to this, sequence components calculation in both two-phase and three-phase is given, for the case of unbalanced system voltage. Then, a classification of different Quadrature Signal Generation (QSG) techniques used for grid synchronization is given. A complete quadrature signal generation procedure based on SOGI for the purpose of grid synchronization is described in detail. Application of the SOGI for different purpose is also given afterward. Finally, complete illustration and experimental results for both 1-phase and 3-phase PLL are presented to check the usefulness of the algorithm

### **3.1 Introduction**

There is a requirement of robust grid condition monitoring system for DPGS, in order to maintain the quality and safety as per our normal requirement [7-11]. Amplitude, phase angle and frequency of the utility grid need to be identified faster with a higher accuracy, in order to generate reference signal. This reference signal needs to satisfy the demands, regarding the operational margins. As per the standard IEC61727-2002, for interfacing the photo voltaic systems [9], the operational limit of grid frequency and amplitude are displayed in Figure1. As per the Figure.1, normal operational area is defined. This area starts 0.85 p.u. amplitude to 1.10 p.u. amplitude, where frequency defined in the range of  $\pm 1$  Hz around the nominal frequency of the voltage. The system may not affect continuously by normal grid condition, abnormalities also can arise on the grid. So there is a need of response from the grid connected DPGS. The DPGS has to stop, to empower the utility network within the given time limit, when amplitude and frequency surpass the limiting region. The trip time of 0.05 seconds is required for most restrictive requirement, when the grid voltage amplitude exceeded the 1.35 p.u. limit. In order to satisfy these requirements, a robust and fast grid voltage condition monitoring system is required.

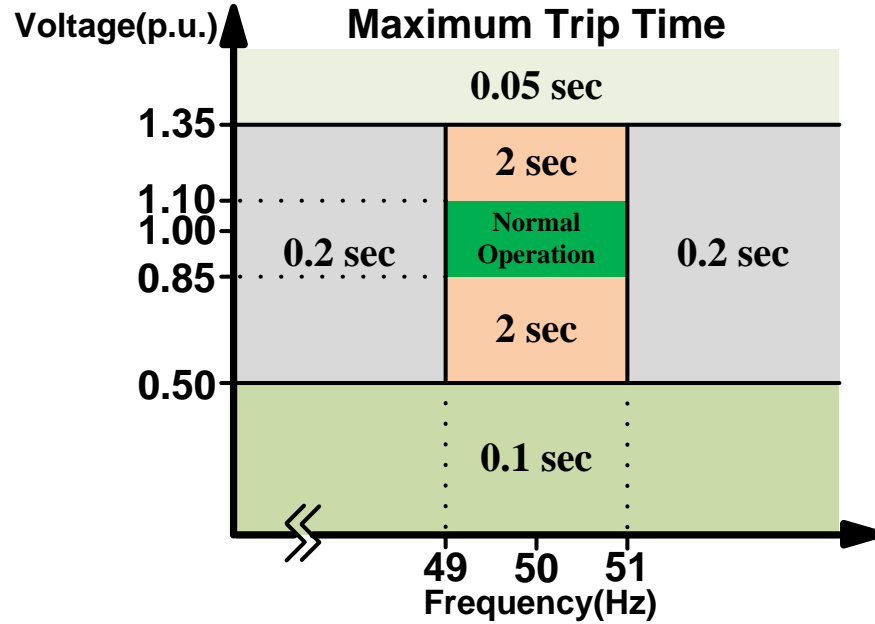


**Figure.1. Maximum trip time with respect to both voltage amplitude and frequency, according to the standard IEC61727-2002, especially for PV systems.**

For unison operation of DPGS with the utility grid, phase angle ( $\omega t$ ) is generally used. Furthermore, the phase angle detection could also use for anti-islanding detection [16]. Angular frequency ( $\omega$ ) is necessary for the case of frequency unbalance, where it is used for under/over frequency finding process. This also provides info to control system, because some equipment need the value of frequency to work accordingly. For under/over voltage detection and power feed forward loop, voltage magnitude is essential. Furthermore, information about harmonics content is also needed for some specific operation. For example, passive anti-islanding methods [16] and active power filters applications [17, 18] are largely depend upon the harmonic information.

This chapter centers on the estimation of phase angle of grid voltage. In the coming section, a small overview of different technique used for grid voltage monitoring is given.

### 3.2 Overview of Grid Voltage Monitoring System

For monitoring the grid voltage, various methods using different techniques are presented in the literatures. But some methods are leading to confusion, due to they have not categorized always. So, to get clarity in this aspect, techniques used for grid voltage monitoring are categorized as per Figure.2. It is mainly split into two categories, specifically methods based on Zero-Crossing Detection (ZCD) and Phase Locked Loop (PLL). Phase Locked Loop based

approaches are having phase controller, where Zero-Crossing Detection approaches don't have the phase controller. Furthermore, PLL techniques are classified in to three different categories, namely ZCD based PLL, Arctangent Function ( $\tan^{-1}$ ) based PLL and Park Transformation based PLL. In coming sections, these techniques are explained in more detail.

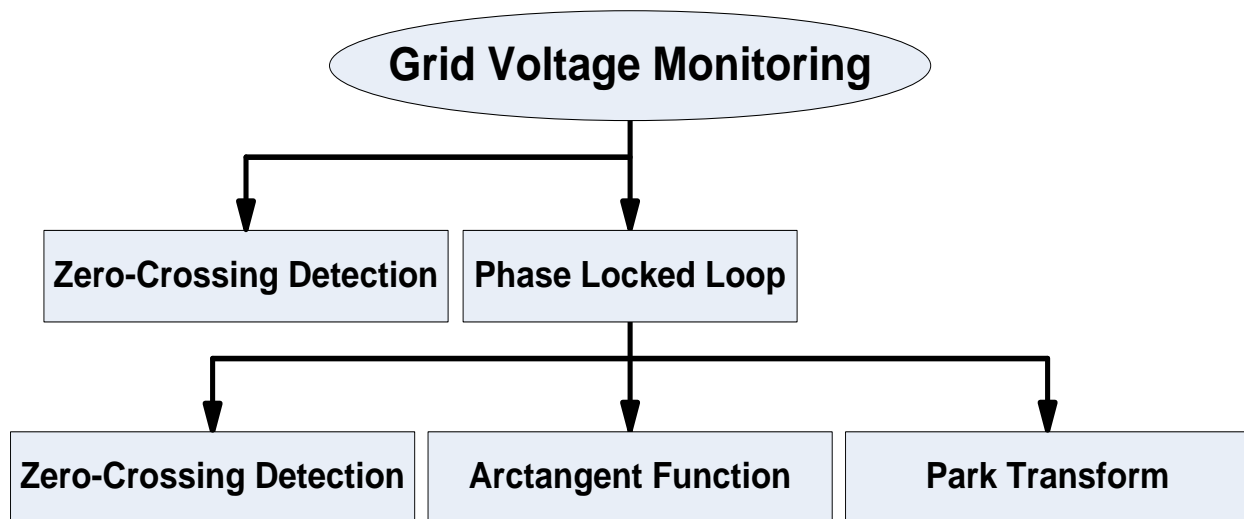


Figure.2. Classification of the grid voltage monitoring techniques for DPGS.

### 3.2.1 Voltage monitoring based on ZCD

Obtaining zero-crossing point of grid voltage is a simple approach for grid synchronization [19-21]. When the input supply voltage passes through the Zero Crossing Detector (ZCD), it gives rise pulses, in completion of each half cycle. The time duration measured between two consecutive pulses, is half of the fundamental time period. So dividing the measured time interval in between two consecutive samples, with respect to  $\pi$ , we will be able to get the angular frequency ' $\omega$ '. Integrating the angular frequency with respect to time, phase will be extracted. The complete picture is shown in Figure.3.

We are facing two major shortcomings in this method. First one, it is not possible to track the phase in between two detected point, since the zero crossing is avail at every half cycle. So, it is not suitable for fast dynamic response [22]. To overcome the short-comings, some work already has been done, where multiple level crossing detection is used [23]. But still it is not useful, due to its complexity nature. Second one, the notches produced by power device



switching, create problem in conventional ZCD [24]. So this method proves to be unsuitable and complex, where the application requires correct and fast detection of the utility grid voltage.

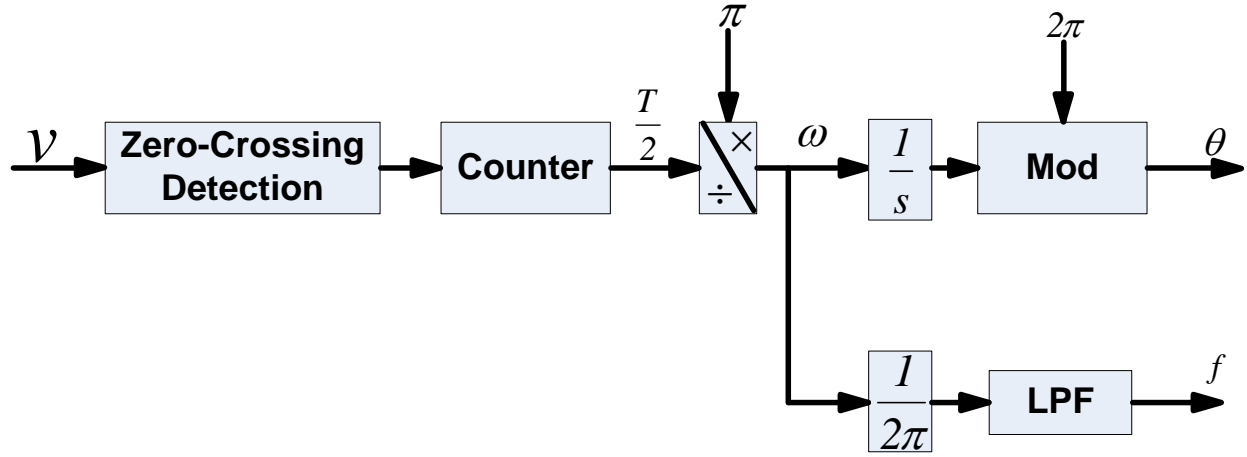


Figure.3 Grid voltage monitoring based on Zero-Crossing Detection

### 3.2.2 Voltage monitoring based on PLL

Now-a-days, there has been a growing concern towards PLL techniques for the grid-side-converter systems [25]. Basically the PLL technique is used in communication network. But as it works efficiently in grid connected converter system [21, 22, 25-32], it need to have more attention for unison operation of inverters. The important task for the PLL is to extract the phase angle of positive sequence input fundamental components. For the case when requirement of reactive power is zero, there is a need to match the output current of inverter with the voltage of PCC. Basically for this purpose, phase angle is much more useful [33]. Apart from phase angle, PLL is also useful to provide amplitude and frequency.

PLL is having a phase comparator, which offers an error signal ( $\varepsilon_\theta$ ). Then this is fed to PI controller. As shown in Figure.4, initial frequency value ( $\omega_l$ ) with addition to PI controller output, results the estimated frequency ( $\omega^*$ ) of the utility voltage. Then, by simply taking the integral of frequency, phase is extracted ( $\theta^*$ ). To offer the phase reference to phase-comparator, these methods could be used: the arctangent function, the ZCD or the Park Transformation.

### 3.2.2.1 Zero Crossing Detection based PLL

This method can also be useful to provide the reference phase angle, to the PLL [21], shown in Figure.4. At every positive slope zero-crossing the integrator is reset to zero and at every negative slope zero crossing the integrator is reset to  $\pi$ . By this way, it is able to deliver the phase angle reference to the Phase Locked Loop. The disadvantages are similar to those ZCD.

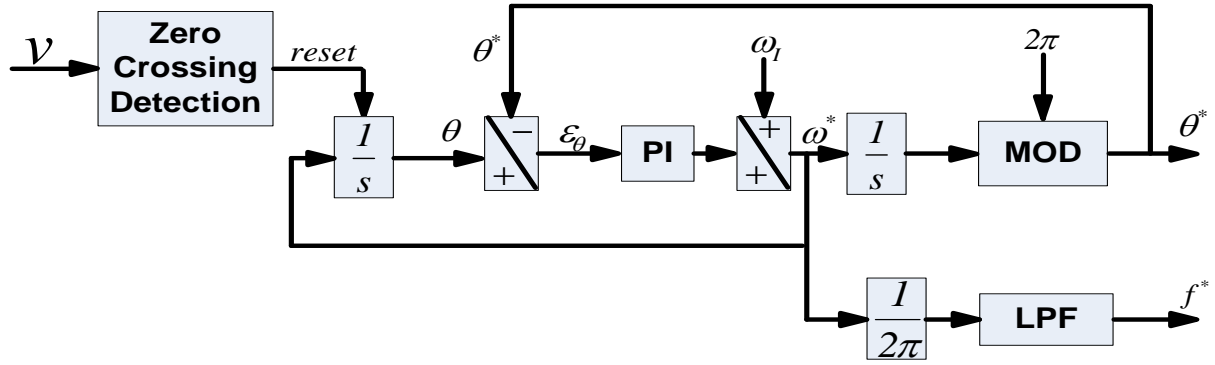


Figure.4. PLL structure by the use of Zero Crossing Detection

### 3.2.2.2 Arctangent Function based PLL

It is another method for phase angle detection and fundamental frequency estimation of the utility grid [21-34]. As shown in Figure.5, a quadrature signal generator is required to apply this technique. It also has two basic disadvantages. In case of distorted grid condition, it requires advanced filter techniques to extract the proper phase and frequency of the grid voltage [35]. Secondly, it is facing difficulties in implication, due to the presence of division-by-zero. So, it is also not the suitable choice for grid side converter.

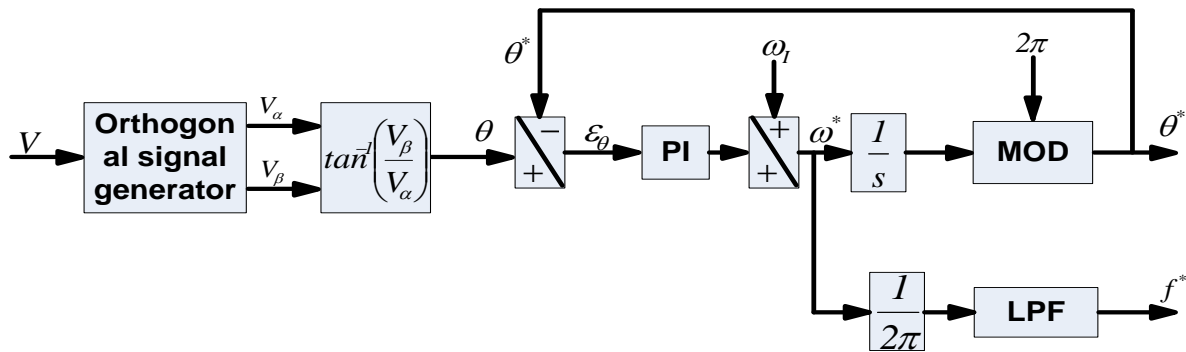


Figure.5. PLL structure by the use of Arctangent Function

### 3.2.2.3 Park's Transform based PLL

PLL based on Park's transformation, is the most used technique for phase extraction. As shown in Figure.6, it also need quadrature signal generator similar to the case of Arctangent based PLL.

To understand it deeply, let's take a sinusoidal signal 'V'.

$$\text{Where } V = A \sin \theta \quad (1)$$

By the use of QSG (quadrature signal generator), we get the signals as  $V_\alpha$  and  $V_\beta$ . Where  $V_\alpha$  and  $V_\beta$  are the in-phase and quadrature components respectively.

$$\text{In matrix form } \begin{bmatrix} V_\alpha \\ V_\beta \end{bmatrix} = \begin{bmatrix} A \sin \theta \\ A \cos \theta \end{bmatrix} \quad (2)$$

By transforming it to the d-q reference frame using Park's transformation matrix 'P', we get  $V_d$  and  $V_q$ .

$$\text{In matrix form, } \begin{bmatrix} V_d \\ V_q \end{bmatrix} = [P] \begin{bmatrix} V_\alpha \\ V_\beta \end{bmatrix} \quad (3)$$

$$\text{Where } P = \begin{bmatrix} \cos \theta^* & -\sin \theta^* \\ \sin \theta^* & \cos \theta^* \end{bmatrix} \quad (4)$$

Here  $\theta^*$  is the extracted phase of the PLL.

$$\text{So finally, } V_d = V_\alpha \cos \theta^* - V_\beta \sin \theta^* \quad (5)$$

$$\Rightarrow V_d = A \sin \theta \cdot \cos \theta^* - A \cos \theta \cdot \sin \theta^*$$

$$\Rightarrow V_d = A \sin(\theta - \theta^*) \quad (6)$$

For normalized grid voltage,

$$V_d = \sin(\theta - \theta^*) \quad (7)$$

As of (7), to get the phase angle  $\theta^*$  as the input phase of the signal  $\theta$ ,  $V_d$  should become zero. So Figure.6 is a feedback system, which is constructed upon this logic. Here extracted phase  $\theta^*$  always follow the input phase  $\theta$ . Presence of PI controller makes the error value  $V_d$  to become zero.

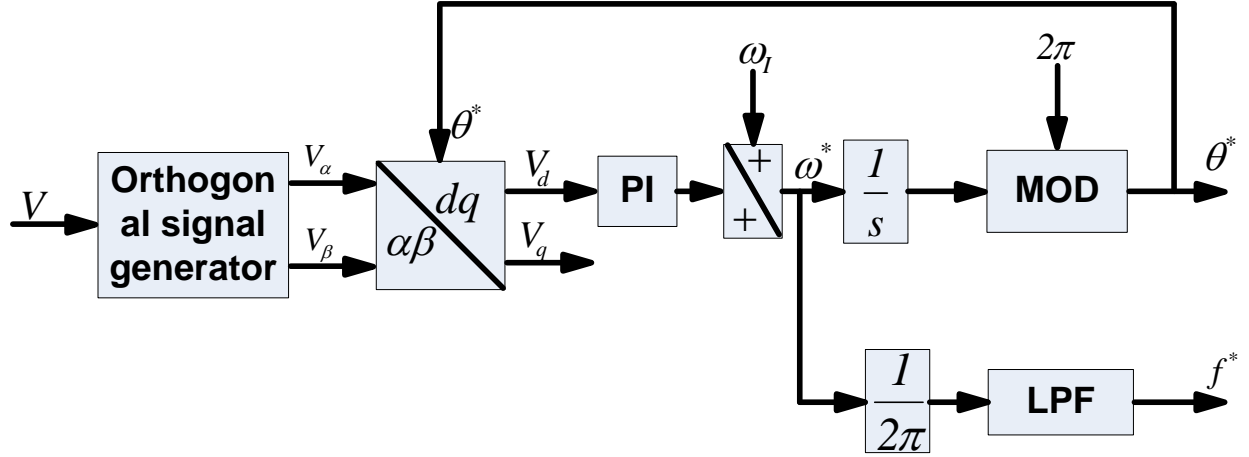


Figure.6. PLL structure by the use of Park's Transformation matrix

Unlike to single phase system, in three phase system the orthogonal component of voltage is generated by Clarke's transformation. For the purpose of understanding, let's take a balanced three phase supply ' $V_{abc}$ '

$$V_a = A \sin \theta$$

$$\text{Where, } V_b = A \sin\left(\theta - \frac{2\pi}{3}\right) \quad (8)$$

$$V_c = A \sin\left(\theta + \frac{2\pi}{3}\right)$$

Transforming the input voltage from a-b-c reference frame to two-phase stationary reference frame values  $V_{\alpha\beta}$ , we get two orthogonal components  $V_\alpha$  and  $V_\beta$ . This is shown in (9).

$$\begin{bmatrix} V_\alpha \\ V_\beta \end{bmatrix} = [T_{\alpha\beta}] \begin{bmatrix} V_a \\ V_b \\ V_c \end{bmatrix} \quad (9)$$

$$\text{Where, } [T_{\alpha\beta}] = \frac{2}{3} \begin{bmatrix} 1 & -\frac{1}{2} & -\frac{1}{2} \\ 0 & \frac{\sqrt{3}}{2} & \frac{\sqrt{3}}{2} \end{bmatrix} \quad (10)$$

But for unbalanced supply voltage, it is desired to calculate the positive sequence fundamental components. So in the following section, we are going to discuss about the sequence components calculation in both three phase and two phase system.

### 3.3 Sequence Components Separation

Procedure applied in previous section is only applicable for single phase system or a balanced 3-phase system. However for the unbalanced grid voltage it is not applicable, due to the existence of -ve sequence components. So for unbalanced 3-phase supply, sequence separation is a necessary choice. But it should be keep in mind, for the operation of grid-connected converter only +ve sequence components are sufficient. This can be done either in 3-phase domain or in 2-phase domain. We are going to extract the sequence components in both 3-phase and 2-phase system, in coming section.

#### 3.3.1 Sequence components separation in three phase system

Due to the arise of unbalanced condition from unequal voltage sources or loads, Charles Legeyt Fortescue presented a paper, for the purpose of calculating both +ve and -ve sequence components. Basing upon this technique the three phase unbalanced supply is divided into three different components, namely: +ve sequence, -ve sequence and zero sequence component. So by applying the C.L. Fortescue method in three phase system, we get positive and negative sequence components as follows (11a) and (11b).

$$\begin{bmatrix} V_a^+ \\ V_b^+ \\ V_c^+ \end{bmatrix} = \frac{1}{3} \begin{bmatrix} 1 & \lambda & \lambda^2 \\ \lambda^2 & 1 & \lambda \\ \lambda & \lambda^2 & 1 \end{bmatrix} \begin{bmatrix} V_a \\ V_b \\ V_c \end{bmatrix} \quad (11a)$$

$$\begin{bmatrix} V_a^- \\ V_b^- \\ V_c^- \end{bmatrix} = \frac{1}{3} \begin{bmatrix} 1 & \lambda^2 & \lambda \\ \lambda & 1 & \lambda^2 \\ \lambda^2 & \lambda & 1 \end{bmatrix} \begin{bmatrix} V_a \\ V_b \\ V_c \end{bmatrix} \quad (11b)$$

Where  $V_{abc}^+$  and  $V_{abc}^-$  are +ve and -ve sequence components of unbalanced 3-phase supply  $V_{abc}$  respectively. And here  $\lambda = 1\angle 120^\circ$  used as a phase advancing operator. But as in PLL we go for three-phase to two-phase conversion, it is better to choose sequence separation in two-phase system, which give less computation with respect to three-phase system.

### 3.3.2 Sequence components separation in two phase system

As we know from previous section that three phase system put more calculation burden and complexity in sequence components estimation, so we put interest in two phase system. We know that, unbalanced signal consists of two space vector, which are rotating in opposite to each other [36]. The space vectors which rotate in the same direction of input supply known as +ve sequence components and the other are -ve sequence components. Both +ve and -ve vector orientation are shown in Figure.7. In general the unbalanced space vector can be decomposed as (12a) and (12b).

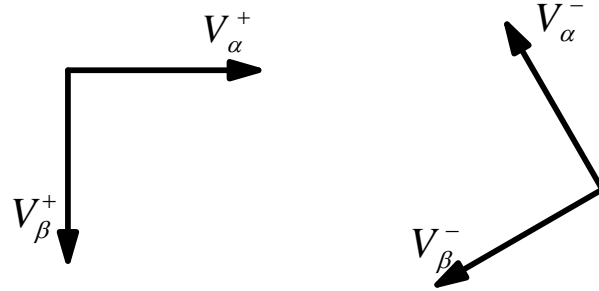


**Figure.7. Positive and negative sequence voltage orientation**

$$V_\alpha = V_\alpha^+ + V_\alpha^- \quad (12a)$$

$$V_\beta = V_\beta^+ + V_\beta^- \quad (12b)$$

From Figure.7, we get

$$V_\beta^+ = q \cdot V_\alpha^+ \quad (13a)$$

$$V_\beta^- = -q \cdot V_\alpha^- \quad (13b)$$

Where ‘q’ is a phase shift operator, having  $90^\circ$  phase delay. i.e  $q = 1\angle -90^\circ$ .

Taking the value of  $V_\beta^+$  and  $V_\beta^-$  from (13) and putting it in (12a), we get (14).

$$V_\beta = qV_\alpha^+ - qV_\alpha^- \quad (14)$$

Multiplying ‘q’ in both sides of (14),

$$qV_\beta = -V_\alpha^+ + V_\alpha^- \quad (15)$$

Solving (12a) and (15),

$$\begin{bmatrix} V_\alpha^+ \\ V_\alpha^- \end{bmatrix} = \frac{1}{2} \begin{bmatrix} 1 & -q \\ 1 & q \end{bmatrix} \begin{bmatrix} V_\alpha \\ V_\beta \end{bmatrix} \quad (16a)$$

As of (13), for the calculation of both +ve and –ve sequence components of ‘ $V_\beta$ ’, simply multiply ‘q’ into  $V_\alpha^+$  and multiply ‘-q’ into ‘ $V_\alpha^-$ ’ respectively.

$$\begin{bmatrix} V_\beta^+ \\ V_\beta^- \end{bmatrix} = \frac{1}{2} \begin{bmatrix} q & 1 \\ -q & 1 \end{bmatrix} \begin{bmatrix} V_\alpha \\ V_\beta \end{bmatrix} \quad (16b)$$

Rearranging the +Ve and -Ve sequence components separately, we get (17).

$$\begin{bmatrix} V_\alpha^+ \\ V_\beta^+ \end{bmatrix} = \frac{1}{2} \begin{bmatrix} 1 & -q \\ q & 1 \end{bmatrix} \begin{bmatrix} V_\alpha \\ V_\beta \end{bmatrix} \quad (17a)$$

$$\begin{bmatrix} V_\alpha^- \\ V_\beta^- \end{bmatrix} = \frac{1}{2} \begin{bmatrix} 1 & q \\ -q & 1 \end{bmatrix} \begin{bmatrix} V_\alpha \\ V_\beta \end{bmatrix} \quad (17b)$$

As of Equation (17), for the calculation of sequence components, quadrature signal generator is the essential requirement. So, in coming section, various techniques used for generating the orthogonal voltage are given.

### 3.4 Overview of QSG Technique

To generate the quadrature signal from a single phase system, numerous methods are elaborated in technical literatures. Also some comparisons are given in [21, 25, 37]. The Quadrature Signal Generator (QSG) offers orthogonal signal ‘qV’ of the input signal ‘V’. For better understanding,

$$\text{Let the input voltage} \quad V = \sin(2\pi.50.t) \quad (18a)$$

$$\text{So the Quadrature output} \quad qV = -\cos(2\pi.50.t) \quad (18b)$$

Both the input and quadrature signals are shown in Figure.8.

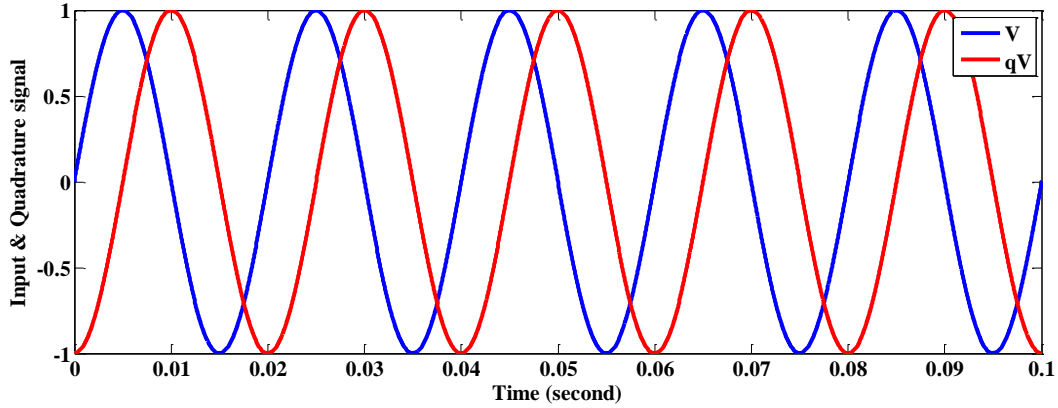


Figure.8. Input and Quadrature signal generated by QSG

Later in this thesis, we take the analogies as given in (19), for the Park's Transformation and Arctangent method used in PLL.

$$V_\alpha = V = \sin(2\pi.50.t) \quad (19a)$$

$$V_\beta = qV = -\cos(2\pi.50.t) \quad (19b)$$

For producing the quadrature voltage, numerous methods are given in coming section.



### 3.4.1 Transport delay based QSG

This is the easiest method to create a orthogonal signal, in both understanding and implementation point of view. In order to get the orthogonal signal, the buffer size is fixed to  $1/4^{th}$  of the N. Here N is the number of samples per a complete cycle. Here the orthogonal component only could be generated by  $90^\circ$  phase delay. Figure.9 shows the complete block diagram of Transport delay based orthogonal signal generator, where Figure.10 shows the simulation output. As shown in Figure.10, the adopted data having no simultaneity [38, 39]. I.e from zero second to 0.005second, the quadrature signal showing zero output. For a 50Hz signal, time need to detect the orthogonal component is 0.005second. So it is facing difficulty to meet the real time request [40, 41]. In order to overcome this shortcoming, another method is given in next section.

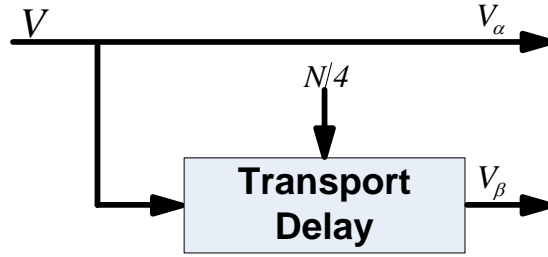


Figure.9. QSG constructed upon Transport Delay

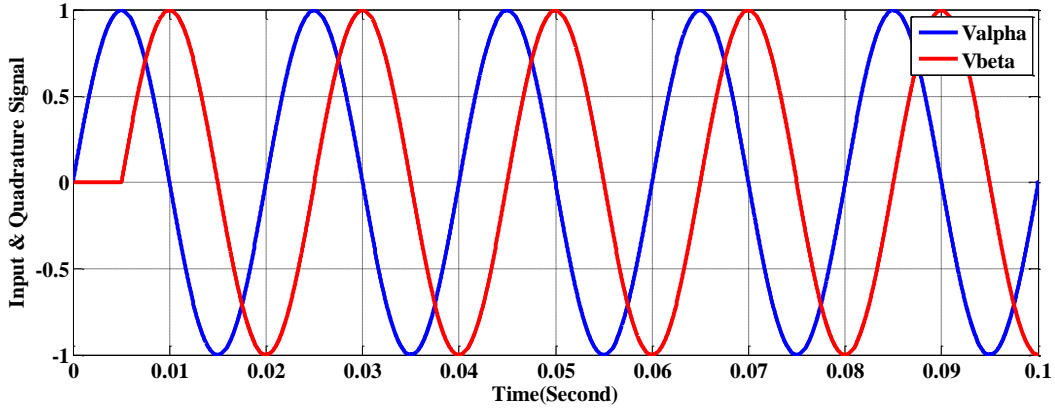


Figure.10. Input (blue) and Quadrature signal (red)

### 3.4.2 Sampling and trigonometric function based QSG

By the use of trigonometric function and sampling delay, orthogonal signal can be generated [42]. The shortcoming observed in previous section is mitigating by this approach. Figure.11 shows, the complete block diagram of sampling and trigonometric function based QSG.

Before constructing the orthogonal signal generator, a small elaboration is given.

Let us take the input signal,  $V = A \sin(\omega t + \theta)$ , which is nothing but the same ' $V_\alpha$ '. Here ' $A$ ' is amplitude of input signal and ' $\omega$ ' is the angular frequency. After putting a delay time of ' $\tau$ ' to the input signal ' $V$ ', a phase shift of ' $\gamma$ ' is done. This signal is termed as ' $V_s$ '.

$$V_s = A \sin(\omega t + \theta - \gamma) \quad (20)$$

Where  $\gamma = \omega \tau$

Expanding ' $V_s$ ',

$$V_s = A \sin(\omega t + \theta) \cos(-\gamma) + A \cos(\omega t + \theta) \sin(-\gamma) \quad (21)$$

From Equation (21),

$$V_\beta = -A \cos(\omega t + \theta) = \frac{A \sin(\omega t + \theta) \cos(-\gamma) - V_s}{\sin(-\gamma)} \quad (22)$$

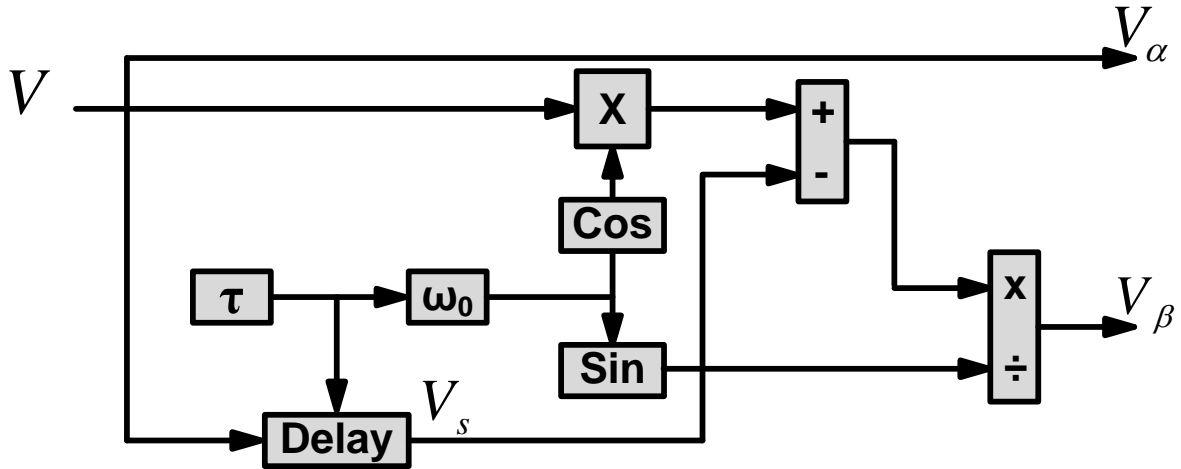


Figure.11. Quadrature signal generator based on trigonometric function and sampling delay

Unlike the detection time requirement of 5ms for 50 Hz signal in the previous method, here the detection time is not a fixed value. The detection time is totally depend upon the value of ' $\tau$ '. Smaller the value of delay time ' $\tau$ ', lesser is the amount of delay in detection of quadrature signal. In order to get better result, this delay time should be smaller. As of Figure.12, this is clearly shown that, detection of quadrature component is faster than the previous case.

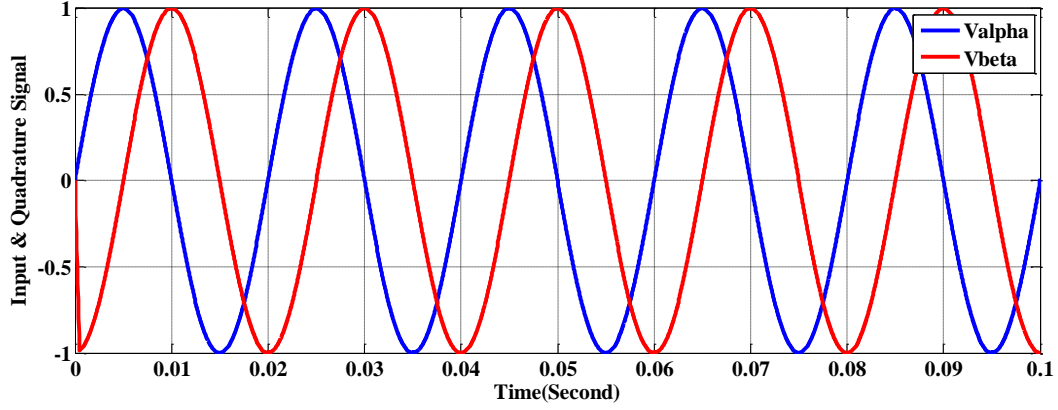


Figure.12. Input (blue) and Quadrature (red) signal generated by sampling and trigonometric function based QSG

### 3.4.3 Estimated phase angle and amplitude based QSG

A very simple QSG system is given in Figure.13. Here, for the generation of quadrature signal, amplitude and phase angle must be known to the user. Then simply taking the cosine ( $\cos$ ) of the phase angle ( $\theta$ ) and multiplied by negative of amplitude ( $-A$ ), quadrature signal is generated. As shown in Figure.13, a sinusoidal signal is given to the single phase PLL (23), which is used to generate the phase angle ( $\theta$ ) and magnitude ( $A$ ) of the signal.

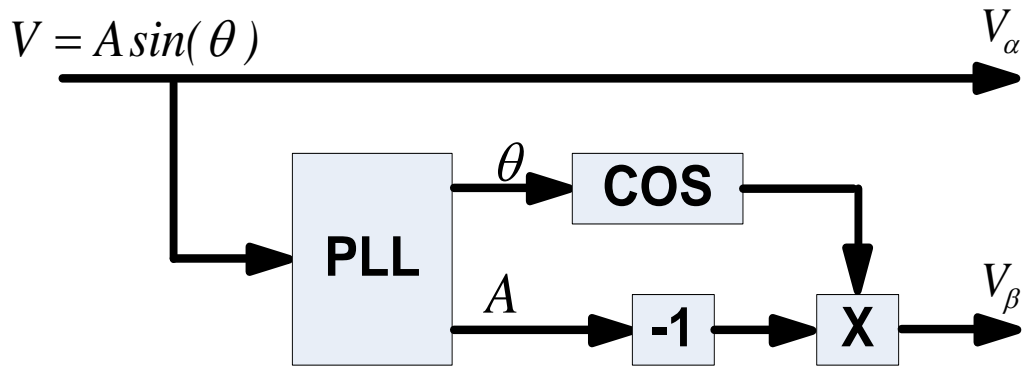
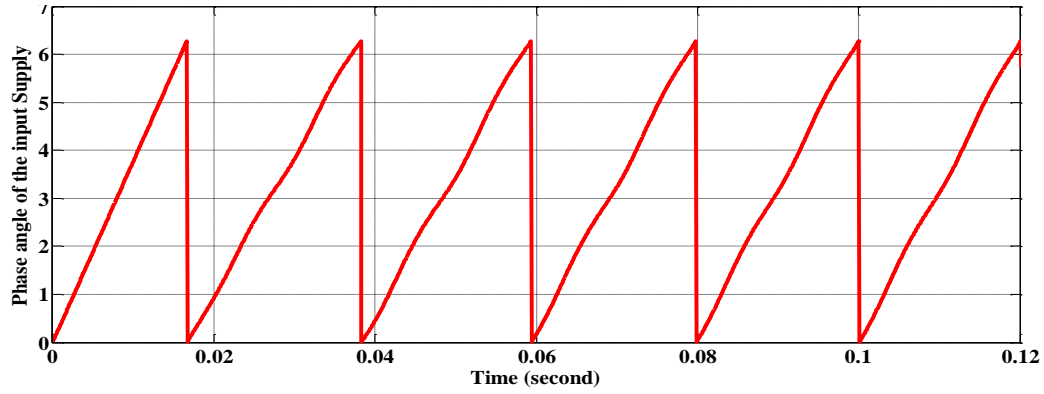
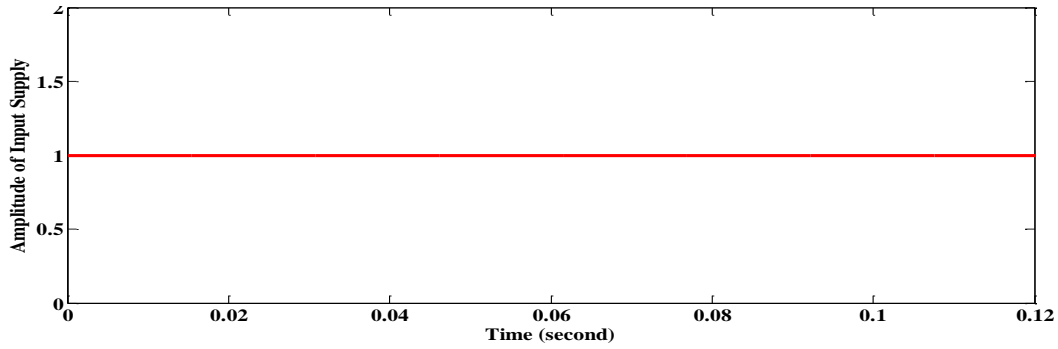


Figure.13. Estimated phase angle and amplitude based QSG



**Figure.14. Phase of input supply, extracted by the single phase PLL**



**Figure.15. Amplitude of input supply, extracted by the single phase PLL**

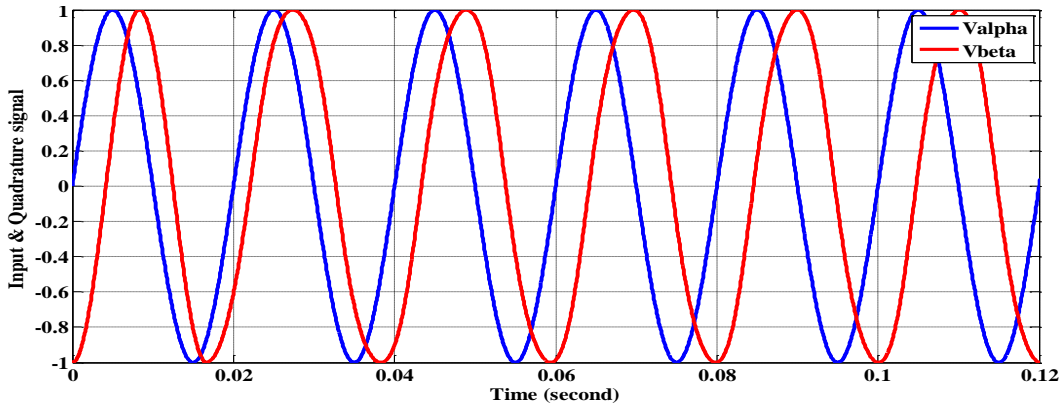


**Figure.16. Input (blue) and Quadrature (red) signal generated by estimated phase angle and amplitude based QSG**

By using this method, orthogonal signal is generated in an easier manner. But it has one major drawback. I.e, the dependency of orthogonal signal generator upon the phase-locked-loop, which gives a poor dynamics to the entire system. Also the PI controller is facing difficulty in tuning, due to the inter-dependent loops in it [21].

### 3.4.4 SOGI based QSG

Apart from all other QSG, SOGI based QSG has become the better choice, due to its multifarious usefulness [32, 43, 44]. It can be useful for the purpose of integrating and band-pass filtering apart from its quadrature signal producing capability. Also this filter is frequency adaptive. Furthermore, a small modification in SOGI based QSG, is useful for frequency estimation [32, 43, 44]. In view of the block diagram of Fig. 17, it is explicitly understood that the output  $qV'$  is obtained by multiplying the resonance frequency  $\omega'$  to the integral of the filtered output  $V'$ . This is given by (23). As this SOGI is employed for quadrature signal generation, it is also called as SOGI-QSG.

$$qV' = \omega' \int V' \cdot dt \quad (23)$$

$$D(s) = \frac{V'(s)}{V(s)} = \frac{k \cdot \omega' \cdot s}{s^2 + k \cdot \omega' \cdot s + \omega'^2} \quad (24a)$$

$$Q(s) = \frac{qV'(s)}{V(s)} = \frac{k \cdot \omega'^2}{s^2 + k \cdot \omega' \cdot s + \omega'^2} \quad (24b)$$

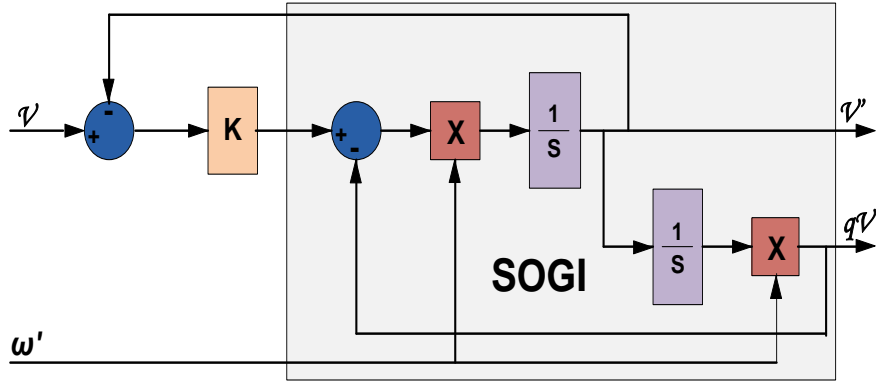


Figure.17. Frequency adaptive second order generalized integrator (SOGI)

The transfer functions for the filtered variable  $V'$  and to the  $90^\circ$  lag filtered variable  $qV'$  to the input variable  $V$  are given by (24).

Here  $\omega'$  is the resonance frequency and  $k$  is the damping factor of SOGI-QSG. Transfer functions of (24) are the best appropriate selection for executing a frequency adaptive filter,

since both the static gain of (24b) and the bandwidth of (24a) are not only independent of center frequency of the filter  $\omega'$ , but also independent of the gain  $k$ . For more selective filtering response, the value of  $k$  should be smaller, but at the moment, it will take longer stabilization time as well. But at  $k = \sqrt{2}$  a useful damped response is achieved. This  $\omega'$  also follows the SOGI resonance frequency.

Taking  $V$  as a sinusoidal signal, the SOGI-QSG output calculated from (24) as follows:

$$V' = DV; qV' = QV$$

As of (24), we found quadrature component  $qV'$  is continuously lag the in-phase filtered voltage  $V'$  by  $90^\circ$ , in spite of any values of  $k$ ,  $\omega$  and  $\omega'$ .

At steady state,  $\omega' = \omega$ ;

Consequently  $|D| = |Q| = 1$ ;

$$\angle D = 0; \angle Q = -\frac{\pi}{2};$$

Thus at steady-state  $V'$  follows the input signal  $V$  with  $0^\circ$  phase-shifts and  $qV'$  follows with  $90^\circ$  lag.

### Frequency Locked Loop (FLL) based on SOGI

From the Figure.18, the transfer-function error signal  $\varepsilon_v$  to the input variable  $V$  is specified (25).

$$E(s) = \frac{\varepsilon_v}{V}(s) = \frac{s^2 + \omega'^2}{s^2 + k \cdot \omega' \cdot s + \omega'^2} \quad (25)$$

In Figure.19,  $E(s)$  and  $Q(s)$  are both combined and plotted in Bode diagram. It is observed, when SOGI resonance frequency higher than the supply frequency ( $\omega' > \omega$ ), the signals  $qV'$  and  $\varepsilon_v$  are in phase. But they are in counter phase, when  $\omega' < \omega$ . Consequently, the frequency error variable ( $\varepsilon_f$ ), which is the product of  $qV'$  and  $\varepsilon_v$ , change its sign according to the largeness of the two frequencies ( $\omega$  and  $\omega'$ ). The  $\varepsilon_f$  value will be negative when  $\omega' < \omega$ ,

positive when  $\omega' > \omega$  and zero, when  $\omega' = \omega$ . By the use of negative gain  $-\gamma$  with integrator, it forces to make the integrator input value zero, by shifting the SOGI resonance frequency  $\omega'$  to the input frequency  $\omega$ . So by the use of SOGI-FLL, frequency of input signal is directly detected.

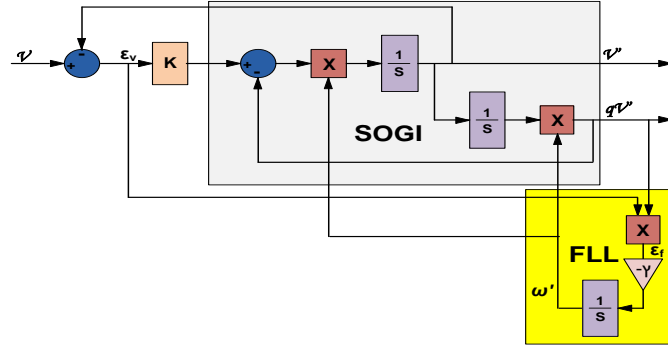


**Figure.18. The SOGI-FLL, for a single-phase grid synchronization system.**

From Figure.20 
$$\varepsilon_f = qV' \cdot \varepsilon_v$$

But 
$$qV' = a \cdot \omega'$$

So we got, 
$$\varepsilon_f = qV' \cdot \varepsilon_v = a \cdot \omega' \cdot \varepsilon_v \quad (26a)$$

Again from figure we found, 
$$\omega' = -\frac{\varepsilon_f \cdot \gamma}{s} \quad (26b)$$

Solving (26a) and (26b), the close loop equation of Figure.20, is presented in (27).

$$\omega' \left( 1 + \frac{a \cdot \varepsilon_v \cdot \gamma}{s} \right) = 0 \quad (27)$$

As per (27), SOGI resonance frequency also satisfies at zero frequency. Then ' $\omega' = 0$ ' is also works as stable operating point, but not as a desired one. The desired value of  $\omega'$  is  $\omega$ . As of (24) and (27), we have two operating point of  $\omega'$ . In order to get the desired value of frequency, a saturation block must need after the FLL output. If the saturation block is having lower limit less than 100rad/s, it shows very sluggish response. But the upper limit only reduces the overshoot. So for better response, the limits need to be closer to the desired value. Keeping frequency fluctuation in sight, the upper limit was taken as 400rad/s and lower limit was 250rad/s.

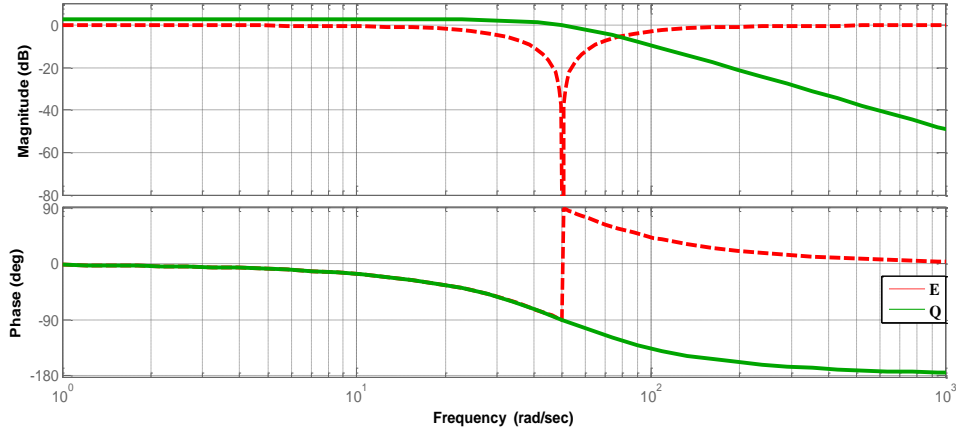


Figure.19. Bode plot of the FLL input variables  $E(s)$  and  $Q(s)$

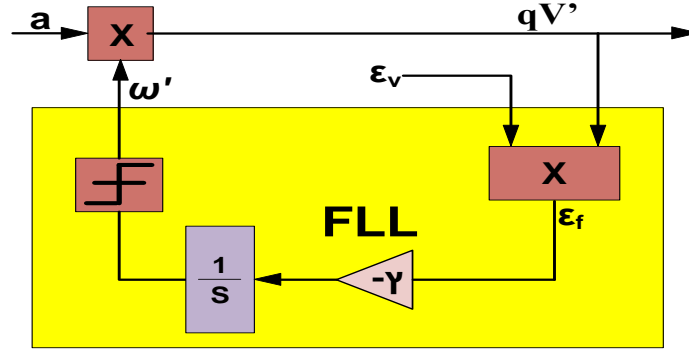


Figure.20. Enlarge view of FLL

By the use of Multiple Second Order Generalized Integrator (M-SOGI), it is useful in extreme distorted grid condition. That mean the harmonic components are also significant in nature. In the upcoming sections, we are going to discuss some single-phase and three-phase PLL. Later we check its performance experimentally by the use of LABVIEW-2010, NI USB-6009 and NI USB-6341.

### 3.5 Single-phase PLL

In this section we are discussing about an advance 1-phase PLL, for the extraction of amplitude, phase angle, frequency of a single phase supply. This PLL is constructed upon SOGI based QSG. So it is best suited for harmonic elimination and fundamental component detection, while introduced to distorted grid condition. Figure.21 shows the complete structure of single-phase PLL. Here a single phase supply of 1 volt and 50Hz is generated by signal generator. This signal is acquired by the use of NI USB-6009, for further programming in computer. As the



measurement system show DC-offset error while measuring, we use an AC-DC estimator block. By the use of this block, we can discard the dc-offset and get only pure ac. The signal generated by the signal generator is not pure ac sinusoidal waveform, it also contain some harmonic, which cause the waveform distortion. After getting the ac waveform, it is fed to the SOGI-QSG.  $dV'$  &  $qV'$  are the filtered in-phase and quadrature components generated by SOGI-QSG. Basing upon  $qV'$  and error signal ' $e$ ', which is same as  $\varepsilon_v$  in (26), (27), a Frequency Locked Loop (FLL) is created. Again the frequency measured by FLL is used for the tuning of SOGI-QSG. Finally the phase is extracted by the use of Park's Transformation based PLL as in  $\delta$  3.2.2.3.

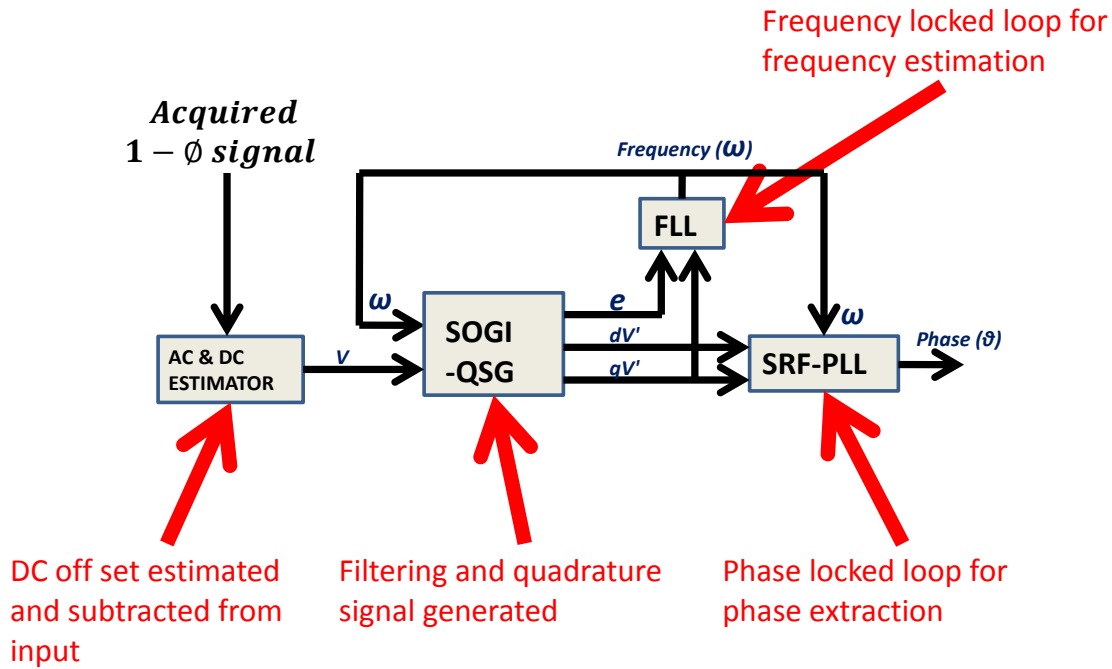


**Figure.21. Complete structure of single-phase PLL**

Figure.22 shows the input supply given to the system. Though the NI USB-6009 is unable to handle more than 10 volt, we generate 1Volt. After acquiring the 1volt ac supply, we multiplied with 230, to represent a 230Volt ac supply. Figure.23 shows the, Filtered in-phase signal ( $dV'$ ) and filtered quadrature signal ( $qV'$ ) generated by SOGI-QSG. As shown in Figure.24, frequency is properly extracted by the Frequency Locked Loop (FLL). It is clearly investigated, that the phase angle of the input fundamental supply voltage is exactly tracked in accordance to input fundamental supply voltage.

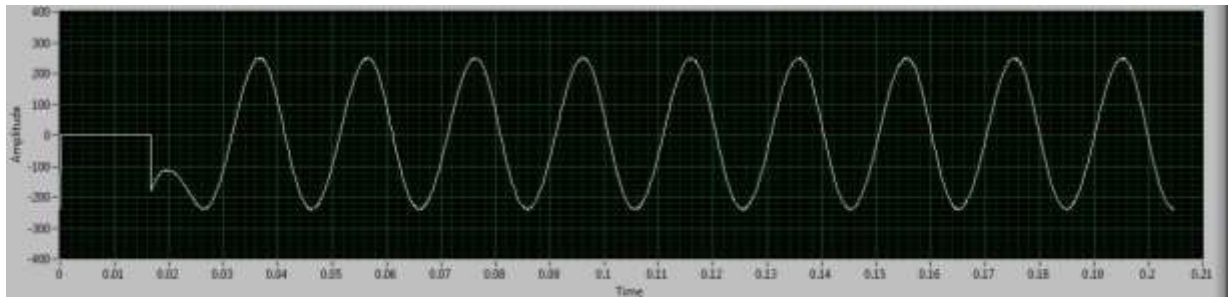


Figure.22. Input supply\*230

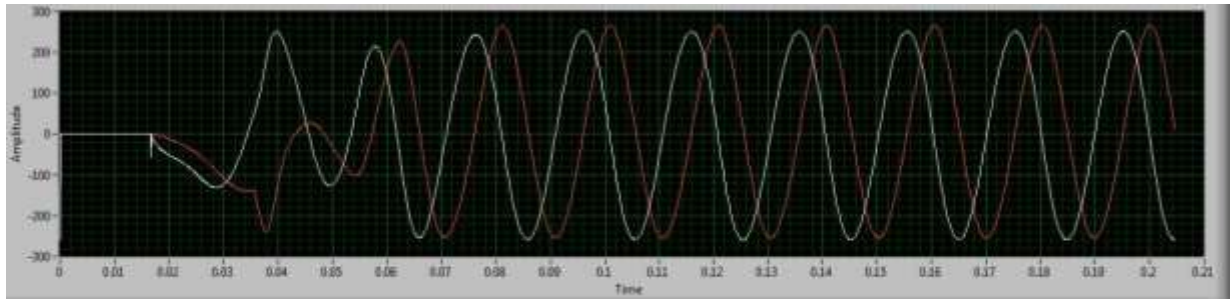


Figure.23. Filtered in-phase signal ( $dV'$ ) and filtered quadrature signal ( $qV'$ ) generated by SOGI-QSG

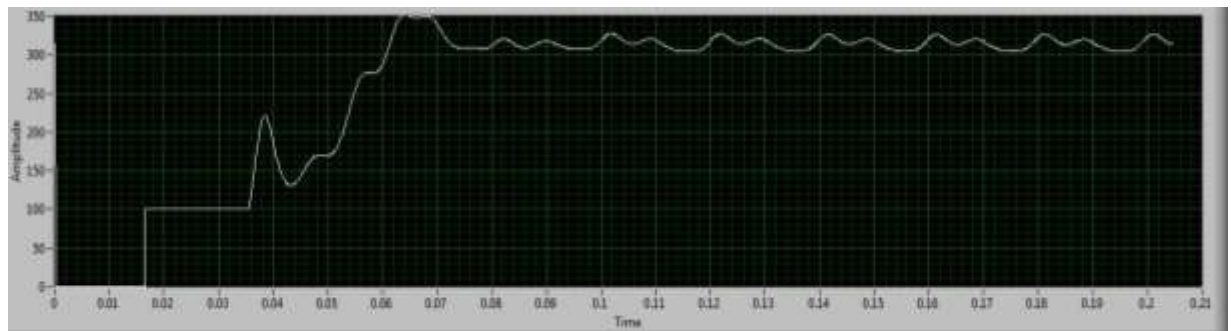


Figure.24. Frequency tracked by SOGI-FLL

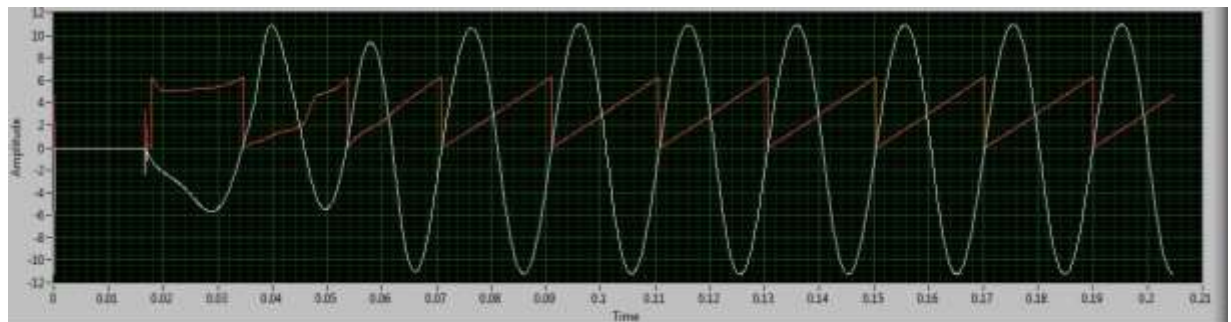


Figure.25. Normalized in-phase component and extracted phase angle of the fundamental supply voltage.

### 3.6 Three-phase PLL

In this section we are going to discuss about an advanced three-phase PLL, where two separate SOGIs are used. These two SOGIs are used for band-pass filtering and sequence components calculation. As per (17), to produce the sequence components of two phase system, quadrature components are required accord with the in-phase components. Here two SOGIs are used to perform this duty, so called Dual-SOGI [43]. The complete structure of the synchronization system is displayed in Figure.26. Here dual-SOGI-QSG (DSOGI-QSG) used in stationary reference frame ( $\alpha\beta$  reference frame), to generate in-phase and quadrature component. These signals are used to generate +Ve sequence generation, by the use of +Ve sequence calculator (PSC). Finally SRF-PLL is used to detect the phase of +Ve sequence fundamental component of the voltage. Here the feed-forward frequency ( $\omega_{ff}$ ) is extracted by the frequency locked loop (FLL).

For experimental verification purpose, a three phase system is taken in consideration.

$$\text{Where, } Phase\_A = 1pu\angle 0^\circ$$

$$Phase\_B = 0.85pu\angle -100^\circ$$

$$Phase\_C = 1.15pu\angle 140^\circ$$

Fundamental frequency of the three-phase unbalanced input supply is 50Hz and having 5<sup>th</sup> and 7<sup>th</sup> order characteristics harmonics. To check the working of FLL, +10Hz is applied at time 0.51s. This +10Hz is taken to check the reliability of the FLL under harder condition and for better resolution. NI USB-6341 have maximum limit to produce two signals at a time. So Clarke's transformation (9) is used to transform the three-phase voltage signal to two-phase.

Then, by the use of NI USB-6341 with LABVIEW, these signals are generated. And acquisitions of these signals are by the use of NI USB-6009, these signals are acquired. Figure.27 shows the complete experimental set-up. As of Figure.26, the positive sequence components are calculated by the use of +ve sequence calculator (PSC). After getting the positive sequence fundamental components, simple SRF-PLL is used to extract the phase angle.

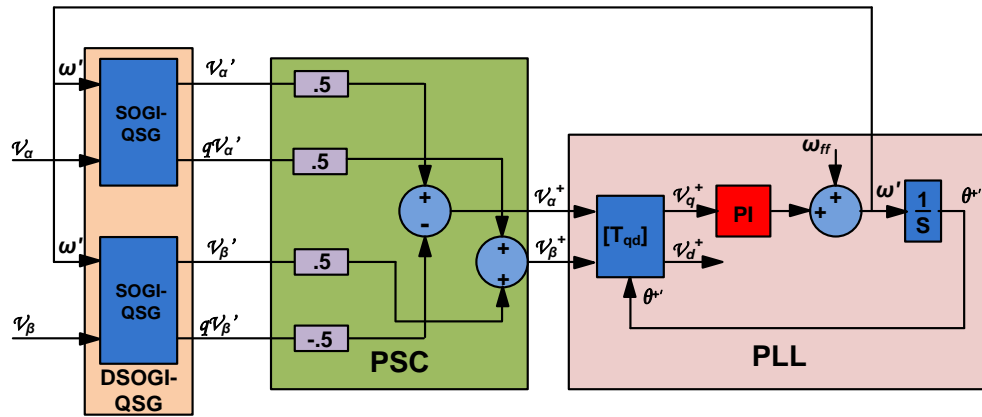


Figure.26. Dual-SOGI synchronization system

Figure.28 shows input supply voltage, after the transformation to stationary ( $\alpha$ - $\beta$ ) reference frame.

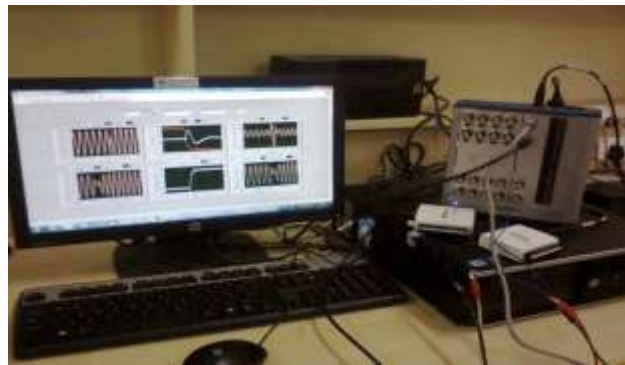
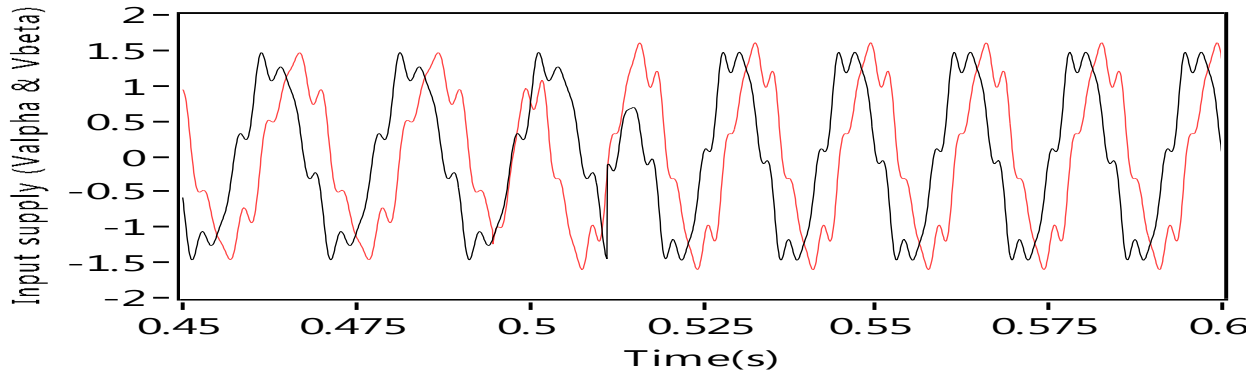
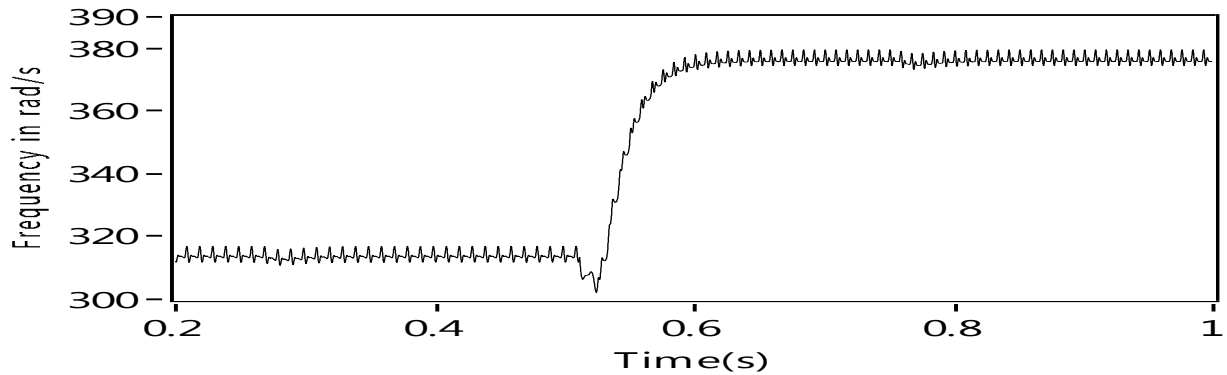


Figure.27. Experimental set-up

As per the results shown in Figure.29 to Figure.31, the robustness of the DSOGI-FLL in case of step change in grid frequency is verified. Figure.29 shows the robustness of the SOGI based FLL, while tracking the step change in frequency from 50Hz to 60Hz. Figure.30 shows positive sequence components estimated by the use of positive sequence calculator (PSC). The main aim of the complete experiment is verified by seeing the Figure.31, where the phase angle of the +Ve sequence fundamental component of Phase-A is extracted. From the Figure.31, it clearly verified that, the phase angle is properly tracked accordingly to the +Ve sequence fundamental component of input 3-phase supply.



**Figure.28. 2-phase input supply ( $\alpha\beta$ )**



**Figure.29. Frequency extracted by SOGI-FLL**

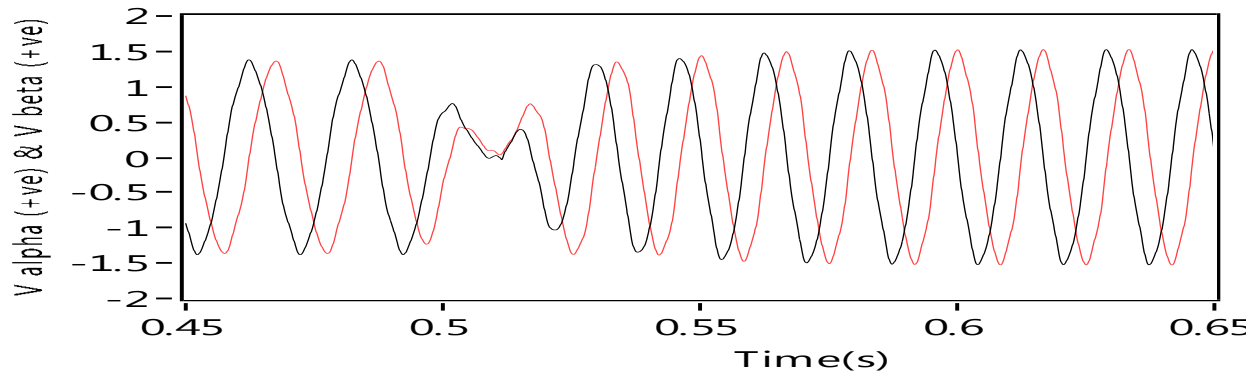


Figure.30. Extracted positive sequence fundamental components ( $V_{\alpha}^{+}, V_{\beta}^{+}$ )

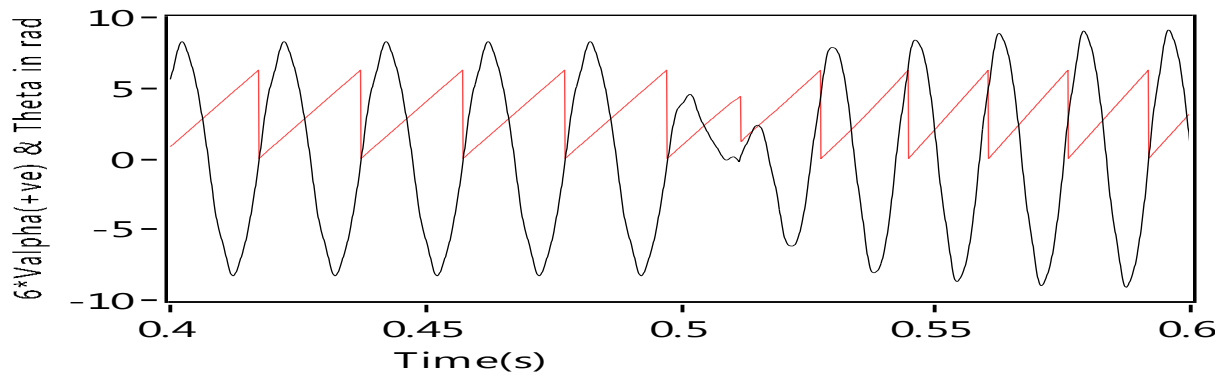


Figure.31. Extracted phase of +VE sequence fundamental component with respect to  $V_{\alpha}^{+} * 5$

## *Chapter 4*

### *(Conclusion)*

# **Conclusion**

## **4.1 Summary**

For the purpose of interfacing an inverter with the grid, the frequency, phase and amplitude of grid voltage are important parameters of consideration. Generally phase extraction is the main motive, and that is also known as grid synchronization.

In the beginning of the thesis, how the sequence components are extracted, a brief discussion both in two-phase and three-phase unbalanced condition is made. For sequence components in two-phase system, the quadrature signal plays a primitive role. So in this thesis a study is made, as to how the quadrature signal is generated and finally it is concluded that, SOGI based quadrature signal generator is the best for this purpose. This is because not only does it help to generate quadrature signal but also it acts as an integrator, a frequency adaptive band pass filter and also a little modification in SOGI helps to estimate the frequency. Finally, the SOGI based single-phase PLL and three-phase PLL are experimentally verified.

## **4.2 Scope for Future Work**

The controller used in SOGI can be designed can be designed using fuzzy logic.



## Bibliography

- [1] "New World Record in Wind Power Capacity," World Wind Energy Association (WWEA), Press Release, January 2007.
- [2] "Renewable 2007 Global Status Report," Renewable Energy Policy Network for the 21<sup>st</sup> Century, December 2007.
- [3] F. Iov, M. Ciobotaru, and F. Blaabjerg, "Power electronics control of wind energy in distributed power systems," in *Proc. of OPTIM*, 2008, pp. XXIX-XLIV.
- [4] F. Blaabjerg and S. Munk-Nielsen, "European Power Electronic conference in Aalborg, Denmark - 1000 participants discussing the future energy technologies," *IEEE Power Electronics Society Newsletter*, vol. 18, pp. 8-10, 2007.
- [5] F. Iov, M. Ciobotaru, D. Sera, R. Teodorescu, and F. Blaabjerg, "Power electronics and control of renewable energy systems," keynote paper, *Proc. of PEDS*, 2007, pp. P-6-P-28.
- [6] J. H. R. Enslin and P. J. M. Heskes, "Harmonic interaction between a large number of distributed power inverters and the distribution network," *Power Electronics, IEEE Transactions on*, vol. 19, pp. 1586-1593, 2004.
- [7] "Automatic disconnection device between a generator and the public low-voltage grid," *German Standard, DIN VDE 0126-1-1*.
- [8] "IEEE recommended practice for utility interface of photovoltaic (PV) systems," *IEEE Std 929-2000*, 2000.
- [9] "Characteristics of the utility interface for photovoltaic (pv) systems," *IEC 61727- 2002*, 2002.
- [10] "IEEE standard for interconnecting distributed resources with electric power systems , " *IEEE Std 1547-2003*, pp. 0\_1-16, 2003.
- [11] "IEEE standard conformance test procedures for equipment interconnecting distributed resources with electric power systems," *IEEE Std 1547.1-2005*, pp. 0\_1-54, 2005.
- [12] Meng, J., "A distributed power generation communication system," *Electrical and Computer Engineering, 2003. IEEE CCECE 2003. Canadian Conference on* , vol.1, no., pp.483,486 vol.1, 4-7 May 2003.\

- [13] Timbus, A.V.; Rodriguez, P.; Teodorescu, R.; Liserre, M.; Blaabjerg, F., "Control Strategies for Distributed Power Generation Systems Operating on Faulty Grid," *Industrial Electronics, 2006 IEEE International Symposium on* , vol.2, no., pp.1601,1607, 9-13 July 2006
- [14] Liao Hongkai; Xu Chenghong; Song Jinghui; Yu Yuexi, "Green power generation technology for distributed power supply," *Electricity Distribution, 2008. CICED 2008. China International Conference on* , vol., no., pp.1,4, 10-13 Dec. 2008
- [15] Yukita, K.; Ichianagi, K.; Goto, Y.; Hirose, K., "A study of electric power quality using storage system in distributed generation," *Electrical Power Quality and Utilisation, 2007. EPQU 2007. 9<sup>th</sup> International Conference on* , vol., no., pp.1,4, 9-11 Oct. 2007
- [16] M. Francesco De, L. Marco, D. A. Antonio, and P. Alberto, "Overview of anti-islanding algorithms for PV systems. Part I: Passive methods," in *Proc. Of PEMCC*, 2006, pp. 1878-1883.
- [17] L. Asiminoaei, F. Blaabjerg, and S. Hansen, "Detection is key - Harmonic detection methods for active power filter applications," *Industry Applications Magazine, IEEE*, vol. 13, pp. 22-33, 2007.
- [18] C. Lascu, L. Asiminoaei, I. Boldea, and F. Blaabjerg, "High performance current controller for selective harmonic compensation in active power filters," *Power Electronics, IEEE Transactions on*, vol. 22, pp. 1826-1835, 2007.
- [19] F. M. Gardner, "Phaselock Techniques," *Publisher: Wiley-Interscience*, vol. 2<sup>nd</sup> edition, ISBN-10: 0471042943, 304 pages, 1979.
- [20] F. Mur, V. Cardenas, J. Vaquero, and S. Martinez, "Phase synchronization and measurement digital systems of AC mains for power converters," in *Proc. Of CIEP*, 1998, pp. 188-194.
- [21] J. W. Choi, Y. K. Kim, and H. G. Kim, "Digital PLL control for single-phase photovoltaic system," *Electric Power Applications, IEE Proceedings*, vol. 153, pp. 40-46, 2006.
- [22] S.-K. Chung, "A phase tracking system for three phase utility interface inverters," *Power Electronics, IEEE Transactions on*, vol. 15, pp. 431-438, 2000.

- [23] C. T. Nguyen and K. Srinivasan, "A new technique for rapid tracking of frequency deviations based on level crossings," *Power Apparatus and Systems, IEEE Transactions on*, vol. PAS-103, pp. 2230-2236, 1984.
- [24] B. P. McGrath, D. G. Holmes, and J. J. H. Galloway, "Power converter line synchronization using a discrete Fourier transform (DFT) based on a variable sample rate," *Power Electronics, IEEE Transactions on*, vol. 20, pp. 877-884, 2005.
- [25] S. M. Silva, B. M. Lopes, B. J. C. Filho, R. P. Campana, and W. C. Bosventura, "Performance evaluation of PLL algorithms for single-phase grid-connected systems," in *Proc. of IAS*, 2004, pp. 2259-2263, vol. 4.
- [26] W. Tsai-Fu, S. Chih-Lung, N. Hung-Shou, and L. Guang-Feng, "A 1phi-3W inverter with grid connection and active power filtering based on nonlinear programming and fast-zero-phase detection algorithm," *Power Electronics, IEEE Transactions on*, vol. 20, pp. 218-226, 2005.
- [27] L. R. Limongi, R. Bojoi, C. Pica, F. Profumo, and A. Tenconi, "Analysis and comparison of phase-locked loop techniques for grid utility applications," in *Proc. of PCC*, 2007, pp. 674-681.
- [28] M. Saitou, N. Matsui, and T. Shimizu, "A control strategy of single-phase active filter using a novel d-q transformation," in *Proc. of IAS*, 2003, pp. 1222-1227, vol.2.
- [29] P. Rodriguez, J. Pou, J. Bergas, J. I. Candela, R. P. Burgos, and D. Boroyevich, "Decoupled double synchronous reference frame PLL for power converters control," *Power Electronics, IEEE Transactions on*, vol. 22, pp. 584-592, 2007.
- [30] M. Ciobotaru, R. Teodorescu, and F. Blaabjerg, "Improved PLL structures for single-phase grid inverters," *Proc. of PELINCEC*, 2005, pp. 6.
- [31] M. Ciobotaru, R. Teodorescu, and F. Blaabjerg, "A new single-phase PLL structure based on second order generalized integrator," *Proc. of PESC*, 2006, pp. 1-6.
- [32] P. Rodriguez, A. Luna, M. Ciobotaru, R. Teodorescu, and F. Blaabjerg, "Advanced grid synchronization system for power converters under unbalanced and distorted operating conditions," *Proc. of IECON*, 2006, pp. 5173- 5178.
- [33] M. Ciobotaru, "Reliable Grid Condition Detection and Control of Single-Phase Distributed Power Generation Systems," PhD Thesis, Aalborg University, Denmark, 2009

- [34] S. Shinnaka, "A new frequency-adaptive phase-estimation method based on a new PLL structure for single-phase signals," in *Proc. of PCC*, 2007, pp. 191-198.
- [35] A. Timbus, M. Liserre, R. Teodorescu, and F. Blaabjerg, "Synchronization methods for three-phase distributed power generation systems. An overview and evaluation," in *Proc. of PESC*, 2005, pp. 2474-2481.
- [36] A. Kulka, "Sensorless Digital Control of Grid Connected Three Phase Converters for Renewable Sources," PhD Thesis, Norwegian University of Science and Technology, Trondheim, Norway, 2009
- [37] J. Salaet, S. Alepuz, A. Gilabert, and J. Bordonau, "Comparison between two methods of DQ transformation for single phase converters control. Application to a 3-level boost rectifier," in *Proc. of PESC*, 2004, pp. 214-220, vol.1.
- [38] M. A. Moreno, J. Usaola. A new balanced harmonic load flow including nonlinear loads modeled with RBF networks. *IEEE Trans. on Power Delivery*. 2004, 9(2):686~693
- [39] G. C. Paap. Symmetrical components in the time domain and their application to power network calculations. *IEEE Transactions on Power Systems*, 2000, 15(2): 522~528
- [40] J. S. Hsu. Instantaneous phasor method for obtaining instantaneous balanced fundamental components for power quality control and continuous diagnostics. *IEEE Transactions on Power Delivery*, 1998, 13(4): 1494~1500
- [41] W. C. Lee, T. K. Lee, D. S. Hyun. A Three-phase Parallel Active Power Filter Operating with PCC Voltage Compensation with Consideration for an unbalanced load. *IEEE Transactions on Power Electronics*. 2002, 17(5): 807~814
- [42] Ma Wenchuan; Zhang Shuo; Shi Nan; Wang Shuwen; Bai Yu; Li Shumin, "Detection Methods of Unbalance Factor and Phase Angle Difference of Positive and Negative Sequence Component of Three-Phase Voltage," *Power and Energy Engineering Conference (APPEEC), 2012 Asia-Pacific*, vol., no., pp.1,4, 27-29 March 2012
- [43] P. Rodriguez, R. Teodorescu, I. Candela, A. V. Timbus, M. Liserre, F. Blaabjerg, "New Positive-Sequence Voltage Detector for Grid Synchronization of Power Converters Under Faulty Grid Conditions," in *Proceedings of the 37th Annual IEEE Power Electronics Specialists Conference, PESC'06*, Jeju, Korea, 18-22 June 2006, 7 pp.

- [44] P. Rodriguez, A. Luna, I. Candela, R. Teodorescu, F. Blaabjerg, "Grid Synchronization of Power Converters using Multiple Second Order Generalized Integrators," in *Proceedings of the 34th Annual Conference of the IEEE Industrial Electronics Society*, Orlando, Florida, USA, 10-13 November 2008, pp. 755-760